Published in final edited form as:
Cancer Prev Res (Phila). 2012 June ; 5(6): 801–809. doi:10.1158/1940-6207.CAPR-11-0555.

Accuracy of *in vivo* multi-modal optical imaging for detection of oral neoplasia

Mark C. Pierce[1,*], **Richard A. Schwarz**[1], **Vijayashree S. Bhattar**[2], **Sharon Mondrik**[1], **Michelle D. Williams**[3], **J. Jack Lee**[4], **Rebecca Richards-Kortum**[1], and **Ann M. Gillenwater**[2]

[1]Rice University, Department of Bioengineering, 6500 Main Street, Houston TX 77030

[2]The University of Texas M. D. Anderson Cancer Center, Dept. of Head & Neck Surgery, 1515 Holcombe Blvd, Houston TX 77030

[3]The University of Texas M. D. Anderson Cancer Center, Dept. of Pathology, 1515 Holcombe Blvd, Houston TX 77030

[4]The University of Texas M. D. Anderson Cancer Center, Dept. of Biostatistics, 1515 Holcombe Blvd, Houston TX 77030

Abstract

If detected early, oral cancer is eminently curable. However, survival rates for oral cancer patients remain low, largely due to late stage diagnosis and subsequent difficulty of treatment. To improve clinicians' ability to detect early disease and to treat advanced cancers, we developed a multi-modal optical imaging system (MMIS) to evaluate tissue *in situ*, at macroscopic and microscopic scales. The MMIS was used to measure anatomical 100 sites in 30 patients, correctly classifying 98% of pathologically confirmed normal tissue sites, and 95% of sites graded as moderate dysplasia, severe dysplasia, or cancer. When used alone, MMIS classification accuracy was 35% for sites determined by pathology as mild dysplasia. However, MMIS measurements correlated with expression of candidate molecular markers in 87% of sites with mild dysplasia. These findings support the ability of non-invasive multi-modal optical imaging to accurately identify neoplastic tissue and pre-malignant lesions. This in turn may have considerable impact on detection and treatment of patients with oral cancer and other epithelial malignancies.

Keywords

Optical imaging; clinical diagnostics; fluorescence imaging; biomarker imaging

Introduction

Oral cancer is one of the ten most common malignancies worldwide, with incidence and mortality rates continuing to rise (1). Despite easy accessibility of the mouth to examination, most patients present with advanced tumors, when treatment is more difficult, more

Corresponding author: Rebecca Richards-Kortum, PhD, rkortum@rice.edu, Phone: 713-348-3823, Fax: 713-348-5877.
*Current address: Rutgers, the State University of New Jersey, Dept. of Biomedical Engineering, 599 Taylor Road, Piscataway, NJ 08854

Potential conflict(s) of interest / Disclosure:
Dr. Richards-Kortum serves as an unpaid scientific advisor to Remicalm LLC, holds patents related to optical diagnostic technologies that have been licensed to Remicalm LLC, and holds minority ownership in Remicalm LLC. Dr. Gillenwater has a minority equity interest in Onconome, Inc., and serves as an unpaid scientific advisor to Remicalm LLC. Dr. Schwarz holds a patent related to optical diagnostic technologies that has been licensed to Remicalm LLC.

expensive, and less successful than early interventions (2). White light examination (WLE), the current approach to screening and identification of oral cancer, has low sensitivity and specificity (3,4). The same techniques are used to determine the extent of lesions in the surgical setting, where an excision margin extending up to 1-centimeter beyond the clinically apparent tumor border is recommended in order to achieve complete removal of neoplastic tissue.

Wide-field autofluorescence imaging (AFI) has emerged as a promising technique to improve the clinician's ability to detect and treat oral neoplasia (3,5–7). AFI illuminates several centimeters of tissue with ultraviolet or blue light, producing visible fluorescence from various tissue components, predominantly stromal collagen. Tissue alterations associated with neoplastic development, such as of loss of collagen integrity and epithelial thickening can lead to a decrease in observed fluorescence intensity, which may be viewed by eye or captured by a camera. In an ongoing study with a commercially available AFI device termed the VELscope, 255 out of 279 (91%) of sites with dysplasia, carcinoma *in situ*, or invasive cancer were detected by loss of fluorescence intensity (8). Significantly, over one-quarter of the sites in the study had pathologic diagnoses of low-grade dysplasia, supporting the potential for AFI to detect early-stage lesions in addition to advanced disease.

AFI may also enable surgeons to better identify the peripheral extent of neoplastic lesions during surgery. In a study by Poh *et al.*, 19 of 20 tumors demonstrated a loss of fluorescence intensity extending 4–25 mm beyond the clinically visible margin (9). 32 of 36 tissue sites within these regions of fluorescence loss showed dysplasia or cancer on histopathology, suggesting that excision margins determined by conventional examination may underestimate the true extent of disease. Long-term data support this hypothesis; a 2009 report from Poh *et al.* (10) presented outcomes on patients who underwent surgical removal of oral lesions between 2004 and 2008, with margins established either by conventional white light examination, or by AFI. 25% of patients in the conventional examination group (7/28) had recurrence of severe dysplasia or cancer, while none of the 32 patients whose margins were guided by fluorescence imaging showed recurrence.

While this loss of autofluorescence intensity appears to be a sensitive indicator of dysplastic or neoplastic alteration (5,11,12), benign conditions including stromal inflammation can mimic this effect on AFI, leading to reduced specificity (13,14). In a recent study of 64 patients at high risk for oral cancer, the sensitivity of the VELscope relative to histology was 100%, but specificity was only 80.8% (15). A separate AFI study in 126 patients with lesions in the oral cavity suspicious for premalignancy resulted in a sensitivity of 84.1% and a specificity of only 15.3% (16). These findings raise concern over the viability of AFI alone to be used as a screening tool for oral dysplasia and cancer, given the potential for large numbers of false positive diagnoses.

In contrast to the macroscopic view provided by wide-field AFI, high-resolution imaging techniques such as confocal microscopy and microendoscopy enable clinicians to visualize *in vivo* many of the same morphologic features used by pathologists to identify dysplastic and neoplastic epithelium. Topical contrast agents such as acetic acid and proflavine solution enhance the appearance of cell nuclei, allowing features such as nuclear crowding and pleomorphism, and nuclear-to-cytoplasm (N/C) ratio, to be qualitatively and quantitatively evaluated in real-time (17–19). By selectively evaluating morphological alterations within the epithelial layer, confounding effects including stromal inflammation may be avoided. However, these high-resolution imaging techniques only interrogate a very small area of tissue and therefore suffer from the same limitation of biopsies and histopathology, namely the potential to miss occult disease due to sampling error.

Given the individual strengths and limitations of wide-field and high-resolution optical imaging techniques, we hypothesized that the combination of these methods in a multi-modal approach may enable detection of oral pre-malignant lesions and cancers with both high sensitivity and specificity. In this study, wide-field autofluorescence imaging and high-resolution microendoscopy were performed in patients undergoing surgery for oral cancer or dysplasia. At each imaged site, a head and neck surgeon provided a clinical impression based on conventional examination, quantitative image-derived metrics were calculated for each modality, and a definitive diagnosis was provided by pathologic assessment.

Materials & Methods

Study population

The study was approved by the Institutional Review Boards of the University of Texas M. D. Anderson Cancer Center and Rice University. 30 patients (16 male and 14 female) over 18 years of age scheduled for surgical resection of clinically visible oral lesions were recruited to the study; all provided written informed consent prior to participation. 6 out of the 30 patients had undergone previous surgery at or near the site(s) measured in this study. The median age of the study group was 70 years (range: 28–95).

Imaging systems

Wide-field autofluorescence and white-light reflectance images of the oral mucosa were acquired with a simplified version of the multispectral digital microscope system reported by Roblyer *et al.* (20) (for technical specifications, see Supplementary Fig. 1a). The second imaging platform used in this study was a high-resolution microendoscope (HRME) system. Technical details on the HRME design have been described previously (21) and are reported in Supplementary Fig. 1b.

Contrast agents

Following wide-field autofluorescence imaging and prior to imaging with the HRME, up to 1 ml of proflavine solution (0.01% w/v in sterile phosphate buffered saline) was applied topically to the oral mucosa with a cotton-tipped applicator. Proflavine is a fluorescent contrast agent which predominantly stains cell nuclei. The optical absorption peak is at a wavelength of 445 nm, with an emission maximum at 515 nm (21). Proflavine is not yet FDA-approved for internal use in the oral cavity, but it has a long history of safe clinical use as a topical antiseptic agent (22), and has also been used as a fluorescent contrast agent in confocal endomicroscopy trials (23). Proflavine is also a component of Triple Dye, a topical antiseptic routinely used in umbilical care in newborns (24). We carried out this study with proflavine under IND status from the FDA; there were no adverse reactions attributed to proflavine noted in any subject participating in the clinical trial.

Study protocol

All subjects were imaged whilst under general anesthesia in the operating room, immediately prior to surgery. The surgeon (AG) first identified regions of interest by standard white light examination, consisting of clinically abnormal sites and one normal appearing site. At this time, before any imaging was performed, each site was described and classified for risk of neoplasia by the surgeon as either *Normal, Abnormal low-risk, Abnormal high-risk*, or *Cancer*, according to the criteria listed in Supplementary Table 1. The surgeon was not blinded to the patient's history when making this assessment, and for the purposes of the study, this designation was termed the "*Clinical impression*". Next, digital autofluorescence and white light images of each site were acquired with the wide-field imaging system, using dimmed room lights to minimize the collection of ambient light.

Proflavine solution was then applied topically to each site selected, followed by placement of the HRME fiber-optic probe onto the mucosal surface. HRME images were recorded with the probe placed at each site, with an additional digital photograph taken showing the location of probe placement for subsequent identification of image and biopsy sites. A 4 mm punch biopsy instrument was used to remove tissue at each imaged site, including the one site which appeared normal by clinical impression. These “normal” sites were selected at locations contralateral to the diseased tissue, whenever possible, in order to match anatomical sites. Specimens were either sent for immediate processing by frozen section, or placed in fixative for standard histopathology processing, according to the clinical discretion of the treating physician. The entire imaging portion of the study was typically completed in 10–15 minutes.

Pathology processing and review

H&E stained sections from all biopsy specimens were reviewed by the study pathologist (MDW), blinded to the results of optical imaging and categorized as either *Normal / Benign, Mild Dysplasia, Moderate Dysplasia, Severe Dysplasia*, or *Cancer* according to the WHO grading system (25). The *Normal / Benign* category contained any site without a diagnosis of dysplasia or cancer, yielding a total of 45 sites, 20 of which exhibited chronic inflammation (18 mild/moderate, 2 severe). Recognizing that the diagnosis of mild dysplasia by H&E alone can be challenging and may be made easier by supplementing with molecular markers, biopsies with an H&E diagnosis of normal or dysplasia (any grade) were additionally evaluated with immunohistochemical staining for the molecular markers Ki-67, p63, and PHH3. Our rationale for selecting these particular markers for evaluation was based upon studies reported in the literature, discussed below. We recognize that Ki-67, p63, and PHH3 may not represent the optimal panel of markers for oral dysplasia or neoplasia, but in the absence of a widely accepted molecular marker for oral cancer / dysplasia, we elected to proceed with these three candidate markers.

Ki-67 is an established marker for cellular proliferation, and is associated with recurrence following resection of oral dysplasia (26). Torres-Rendon *et al.* demonstrated increased expression levels of Ki-67 in oral tissues diagnosed from normal to dysplasia to cancer (27). Ki-67 expression level alone was not significantly different between dysplastic tissues which progressed to cancer and those that did not. However, values obtained by combining Ki-67 expression with additional biomarkers (Mcm2 or geminin) were statistically different, suggesting a role for Ki-67 in predicting progression. Montebugnoli *et al.* reported a prospective study of 47 consecutive patients with oral squamous cell carcinoma (OSCC), evaluating Ki-67 expression in histologically normal tissue distant from the primary tumor. While patients with oral dysplasia were not part of the study, Ki-67 expression alone was shown to be a promising prognostic factor for the disease-free survival rate in OSCC patients (28).

Overexpression of the tumor suppressor homologue p63 has been shown in oral squamous carcinomas (29) and other sites. p63 was also evaluated as a marker of prognosis by Lo Muzio *et al.* in a 2007 study involving 64 OSCC patients (30). While no statistically significant differences were found between p63 expression and age, sex, or tumor stage, patients with p63 overexpression were found to have a poorer survival rate at 72 months (31% survival) than those with normal p63 levels (80%). p63 has also been assessed as a biomarker for predicting oral cancer risk in patients with leukoplakia (31). In a study of 152 patients with oral preneoplastic lesions (OPL’s), significantly more patients with p63 positive lesions went on to develop oral cancers. Moergel *et al.* evaluated p63 as a marker for radiation resistance and overall survival in 33 OSCC patients by determining p63 expression in biopsies prior to surgery (32). All tumors showed increased p63 expression,

with increased resistance to radiation and lower survival for those patients with elevated p63.

Phosphohistone-H3 (PHH3) is a core histone protein, staining for which highlights mitotic figures (33). Taken together, we believe there is good support for the selection of these three biomarkers as candidate biomarkers for oral dysplasia and cancer.

For more information on IHC processing materials and methods, see the Supplementary Information. IHC stained tissue sections from each measurement site were evaluated by the study pathologist and assigned a discrete IHC score for each of the three markers, according to the criteria shown in Supplementary Table 2.

Data analysis

At each anatomical measurement site, quantitative optical information was extracted from images in the following manner: The location of each biopsy site was identified in the corresponding wide-field white-light image by the surgeon (AG). The tissue autofluorescence level at this site was then quantified by calculating the average ratio of red-to-green pixel intensity within a region approximately 4 mm in diameter, centered on the biopsy site. To account for patient-to-patient variability in native tissue autofluorescence intensity, this ratio was normalized by the same parameter measured at a clinically normal appearing site (20). This metric is subsequently referred to as the "*Normalized R/G ratio*".

HRME images of proflavine-stained tissue primarily reveal cell nuclei as discrete bright dots on a dark background. To quantify parameters related to nuclear morphology, image analysis software was written (Matlab R2010b) to automatically identify nuclei in individual HRME images. The area of each nucleus was calculated, enabling the average nuclear-to-cytoplasm area ratio to be calculated for each image. This metric is subsequently referred to as the "*N/C ratio*".

Results

A total of 100 independent sites were imaged and biopsied in 30 patients; the anatomical distribution is reported in Supplementary Table 3. The surgeon's clinical impression and the pathologist's independent diagnosis are provided for each site in Supplementary Table 4. Out of the 30 patients, 15 had a pathology diagnosis of cancer, 14 a diagnosis of dysplasia, and 1 had no pathologic evidence of dysplasia or cancer.

Figure 1 presents examples of white-light examination, wide-field autofluorescence imaging, and high-resolution microendoscope imaging alongside the corresponding histopathology for two different sites on the tongue of a 57-year-old patient. Fig. 1a-d is a site on the anterior tongue; based on conventional white light examination (Fig. 1a) this site was considered normal by clinical impression. The specific measurement site is indicated by the location of the high-resolution fiber-optic probe, seen entering the image from 10 'o clock. When viewed in AFI mode (Fig. 1b) this site appears bright blue in appearance, characteristic of normal oral mucosa. The high-resolution image obtained with the probe placed at this site is shown in Fig. 1c. The field-of-view is a 720 μm wide *en face* view, corresponding to the diameter of the fiber-optic probe in Fig. 1a. Cell nuclei appear as discrete dots, sparsely and evenly distributed throughout the field-of-view, characteristic of normal epithelium and consistent with the histologic diagnosis of "normal" (Fig. 1d). Figure 1e-h presents the left mid-tongue of the same patient. The specific measurement site (indicated in Fig. 1e by the fiber-optic probe) was considered "abnormal, high-risk" by clinical impression. Under AFI, the measurement site (arrow in Fig. 1f) and surrounding tissue exhibited low autofluorescence intensity. With the HRME probe placed at the

measurement site (Fig. 1g), nuclei appeared significantly more crowded and less uniformly spaced than at the “normal” site, consistent with the histologic diagnosis of “severe dysplasia” at this site (Fig. 1h).

The two sites presented in Fig. 1 were instances where clinical impression, wide-field autofluorescence imaging, high-resolution imaging, and pathology diagnosis were all in agreement. In contrast, Fig. 2 presents a case involving the floor-of-mouth in a 43 year old male which appeared normal on clinical examination under white light (Fig. 2a); however, AFI indicated a dark region with distinct loss of intensity, approximately 1 cm in diameter extending to the right of the frenulum (Fig. 2b). High-resolution imaging within this region revealed local variations in sub-cellular morphology, ranging from discrete well-spaced nuclei at the anterior aspect (Fig. 2c, site “1”) to an irregular, crowded appearance of nuclei at the base of the frenulum (Fig. 2d, site “2”). Histopathology sections from these two sites indicated normal mucosa at site “1” (Fig. 2e) and moderate dysplasia at site “2” (Fig. 2f), consistent with the nuclear morphology observed in the HRME images. An additional case illustrating a false positive finding by clinical examination and AFI which appeared normal by HRME and pathology is presented in Supplementary Fig. 2.

For each of the 100 measured sites, loss of autofluorescence in AFI was quantified by the normalized red-to-green intensity ratio; nuclear size and crowding were quantified in HRME images by the nuclear-to-cytoplasm ratio, as described in the Methods section. Figure 3 shows values for all 100 measurement sites, grouped into three pathology categories; open circles indicate a diagnosis of normal / benign, gray triangles indicate mild dysplasia, and closed circles represent diagnoses of moderate dysplasia, severe dysplasia, or cancer. Figure 3a shows the normalized red-to-green autofluorescence intensity ratio at each site; areas with loss of blue-green fluorescence correspond to higher ratio values. A threshold value of 1.38 correctly classified normal sites versus mild / moderate / severe dysplasia or cancer with 87% sensitivity and 76% specificity. While 97% of sites with a diagnosis of moderate dysplasia, severe dysplasia or cancer were correctly classified using this threshold, only 76% of normal sites and 65% of sites with mild dysplasia were correctly classified (Table 1). Figure 3b shows the N/C ratio, measured with the HRME at the same sites as Fig. 3a. Higher N/C ratios result from enlarged or crowded nuclei; a threshold value of 0.142 correctly classified these measurement sites with 84% sensitivity and 71% specificity. Using this threshold, 92% of sites with a diagnosis of moderate dysplasia, severe dysplasia or cancer were correctly classified using this threshold, but only 71% of normal sites and 65% of sites with mild dysplasia were correctly classified. As shown in Fig. 3c, when these AFI and HRME parameters are used together, a single linear threshold correctly classified 98% of normal sites and 95% of sites with moderate / severe dysplasia, or cancer (Table 1). However, Fig. 3 also illustrates that sites with a pathology diagnosis of mild dysplasia (gray triangles) are the most difficult to classify correctly; using multimodal imaging, only 35% of sites with mild dysplasia were correctly classified as abnormal (Table 1). In Fig. 3c, only 2 out of 9 mild dysplasia sites in patients with a cancerous lesion elsewhere in the oral cavity were classified as abnormal by optical imaging. This suggests that when a lesion with mild dysplasia is classified as abnormal by optical imaging, it is an indication of the biology of that specific site, and not a generalized property of patients with oral cancer.

Recent data suggest that in addition to the dysplastic changes apparent in H&E sections under light microscopy, molecular abnormalities may also indicate early precancerous changes in oral lesions (8,10). We hypothesized that there may be a correlation between parameters measured by optical imaging and candidate biomarker expression levels. Biopsy specimens from all sites with a pathology grade of normal ($n = 45$) or dysplasia (mild, moderate, or severe) ($n = 37$) were stained for Ki-67, p63, and PHH3 markers by immunohistochemistry (IHC). Figure 4 shows representative histopathology sections stained

for Ki-67, p63, and PHH3 from two different measurement sites, both of which were graded as mild dysplasia by H&E (Fig. 4a,e). Images in the upper row (Fig. 4a-d) are from a site classified by optical measurements as normal, while the lower row (Fig. 4e-h) are from a site classified as abnormal. In the site classified as normal by optical measurement, Ki-67 and p63 expression is confined to the lower portion of the epithelium (Fig. 4b,c), while these markers extend to the upper portion of the epithelium for the site classified optically as abnormal (Fig. 4f,g). PHH3 staining highlights mitotically dividing cells at the basal layer in Fig. 4d, which is consistent with normal tissue. PHH3 positive cells extending above the basal layer are apparent in Fig. 4h, which is an abnormal finding associated with dysplasia.

Tissue sections were evaluated according to the objective criteria described in Supplementary Table 2, with the mean IHC scores for each pathology grade and each biomarker shown in Fig. 5a. The expression level of each biomarker (reflected in the mean IHC score) exhibited an increase with increasing grade of dysplasia. When the expression of p63 alone is compared to dysplasia grade by H&E, we found that over 75% of sites graded as moderate or severe dysplasia exhibited high p63 expression (Fig. 5b, left group). Interestingly, over 80% of those sites graded as mild dysplasia and classified as “abnormal” by optical measurement also showed high p63 expression, while only 10% of the mild dysplasia sites classified as “normal” by optical measurement exhibited high p63. When the fraction of sites with positive IHC for the complete panel of Ki-67, p63, and PHH3 biomarkers was calculated, we again noted that most sites with high grade dysplasia and mild dysplasia with abnormal classification by optics were also IHC positive (Fig. 5b, right group).

Optical measurement values for the sites with mild dysplasia are shown in Fig. 5c, stratified by p63 expression level. 5 out of 6 sites with high p63 expression are classified as neoplastic based on the optical image parameters. Similarly, 8 out of 9 sites with low p63 expression had optical measurements which group them with sites considered normal by H&E. After stratifying the 15 sites diagnosed as mild dysplasia by pathology according to p63 status, (with low p63 expression considered normal, and high p63 considered abnormal along with moderate dysplasia, severe dysplasia and cancer), we determined the accuracy of classification by each optical imaging system alone, and in combination (Table 1). When stratified by p63 status, the combination of autofluorescence and high resolution imaging correctly classified 87% of sites with a histologic diagnosis of mild dysplasia. When used alone, the multi-modal imaging system (MMIS) classified all sites with 76% sensitivity and 98% specificity. Following stratification of mild dysplasia sites by biomarker status, MMIS classified all 100 measured sites with 93% sensitivity and 96% specificity.

Discussion

Oral cancer presents several unmet clinical challenges which are also common to other organ sites. Better tools are needed to improve screening for early stage disease, to establish clear surgical margins in patients undergoing treatment, and to monitor high-risk and post-surgery patients for development or recurrence of malignant tumors. Macroscopic AFI with laboratory prototypes and commercial devices has been evaluated in multiple studies with varying patient populations (6,7,9) and has demonstrated excellent sensitivity for identifying abnormal tissue through loss of observed autofluorescence intensity. However, there is concern that the technique has poor specificity due to confounding benign conditions, including inflammation (14,34). The consequences of poor diagnostic specificity in a screening tool are serious, including subjecting many patients to unnecessary procedures, which has the added effect of creating alarm among patients and increasing medical costs. Poor specificity in the surgical setting will result in excessive removal of normal tissue beyond the tumor margins, resulting in compromised functional and cosmetic outcomes. The

ideal tissue visualization system will improve both sensitivity and specificity for identification of precancerous lesions and cancer, above that which is currently achieved by white light examination. In addition, improved methods are required to evaluate early stage lesions, particularly those with mild dysplasia; histopathology is currently a poor predictor of risk for progression of these lesions to higher grade disease (35). Therefore, the ability to non-invasively distinguish low-grade sites with a high probability of malignant transformation from those which will naturally regress would truly represent a paradigm shift in clinical cancer care (8).

In the study reported here, quantitative multi-modal optical imaging correctly classified 98% of pathologically confirmed normal tissue sites and 95% of sites graded as moderate dysplasia, severe dysplasia, or cancer. However, only 6 out of 17 (35%) of sites with a pathology grade of mild dysplasia were correctly classified by optical imaging. We evaluated all 37 sites with a pathology diagnosis of dysplasia, for biomarkers whose expression is likely to be modulated during the development of oral neoplasia (27–34). Consistent with these earlier studies, expression levels of Ki-67, PHH3, and p63 were all found to increase with pathologic grade of dysplasia. When the 17 sites with a pathology grade of mild dysplasia were stratified by p63 expression into the pathology “normal” or “abnormal” groups, we found that optical imaging correctly classified the 100 measured sites with 93% sensitivity and 96% specificity. While these findings are encouraging, we acknowledge that the candidate biomarkers used here are not yet established prognostic indicators; long term follow-up of a large, independent cohort of patients is the most rigorous way to establish the accuracy of these, or any other molecular marker(s) in predicting the risk of progression. However, other studies have also suggested that the probability of neoplastic progression may be measured by non-invasive optical imaging methods. Guillaud *et al.* showed that samples with an elevated nuclear phenotypic score (NPS) were more than 10 times more likely to progress than those without (36). This NPS incorporated the maximum nuclear radius, a parameter which is related to the N/C ratio used here. Poh *et al.* found high-risk LOH profiles in 63% of sites exhibiting loss of autofluorescence at resected tumor margins (9). These observations collectively raise the possibility that multi-modal imaging may facilitate *in vivo* detection of molecularly abnormal yet clinically normal tissue, an exciting prospect for advancing translation of molecular tumor classification tests from the lab into actual clinical care.

This study has several important clinical implications. First, the ability to improve detection of oral premalignant lesions would have tremendous impact in the screening setting, by identifying lesions at a stage where less morbid, less expensive, and completely curative treatment can be administered. The ability to objectively discriminate between abnormalities with different biomarker profiles would further impact clinical decision making. Mild dysplasia is particularly challenging for clinicians because it can appear transiently in reaction to inflammation, trauma, or contact allergy, or it can represent the initial stage in the transition of normal mucosa toward high grade dysplasia or cancer (37). For those tissue sites that remain under suspicion and require a biopsy for definitive diagnosis or molecular analysis, optical imaging methods can assist the physician in selecting the most relevant site from which to obtain the tissue specimen. In the surgical setting, delineation of the dysplastic or neoplastic margins is of the utmost importance, given our current understanding of field cancerization and the high rates of recurrence among head and neck cancer patients. Multimodal optical imaging could be used to provide real-time guidance on resection margins, alone or in combination with frozen section pathology.

This study has several strengths, including the use of independent biopsies with blinded pathology review to provide the gold-standard diagnosis at each site measured. The investigation was carried out with a unique cohort of patients with high probability of

dysplasia or cancer, leading to a distribution of pathology diagnosis across the spectrum from normal, through increasing grades of dysplasia, to cancer.

The ultimate objective for diagnostic adjuvants is to be able to predict which patients with potentially malignant disorders are at high risk of progression and to identify those with low risk who will not require aggressive surveillance. Non-invasive multimodal optical imaging classified tissue sites into normal and neoplastic categories with higher sensitivity and specificity than expert clinical impression. While sites with mild dysplasia proved the most difficult to classify by any method, stratification with the candidate biomarker p63 increased the classification accuracy of MMIS at these sites. While molecular abnormalities have traditionally only been identified in resected tissue, the prospect of using optical imaging for real-time, *in vivo* delineation of molecularly damaged mucosa is particularly exciting and warrants further study. This includes establishing a consensus on the appropriate biomarker (or markers) which reliably indicate malignant potential, and then testing optical imaging measurements against these markers in longitudinal studies. Significantly, these principles have potential to be extended to the screening, diagnosis, and treatment of dysplasia and neoplasia in other organs beyond the oral cavity.

Supplementary Material

Refer to Web version on PubMed Central for supplementary material.

Acknowledgments

Financial support: This research was funded by the Cancer Prevention and Research Institute of Texas (CPRIT), grant RP100932, and the US National Institutes of Health, grant R01 EB007594.

References

1. Ferlay, J.; Shin, HR.; Bray, F.; Forman, D.; Mathers, C.; Parkin, DM. Cancer Incidence and Mortality Worldwide: IARC CancerBase No. 10. Lyon, France: International Agency for Research on Cancer; 2010. GLOBOCAN 2008 v1.2.
2. Chen AY, Myers JN. Cancer of the oral cavity. Dis Mon. 2001; 47:275–361. [PubMed: 11477373]
3. Lingen MW, Kalmar JR, Karrison T, Speight PM. Critical evaluation of diagnostic aids for the detection of oral cancer. Oral Oncol. 2008; 44:10–22. [PubMed: 17825602]
4. Thomson PJ. Field change and oral cancer: new evidence for widespread carcinogenesis? Int J Oral Maxillofac Surg. 2002; 31:262–266. [PubMed: 12190131]
5. De Veld DC, Witjes MJ, Sterenborg HJ, Roodenburg JL. The status of *in vivo* autofluorescence spectroscopy and imaging for oral oncology. Oral Oncol. 2005; 41:117–131. [PubMed: 15695112]
6. Lane PM, Gilhuly T, Whitehead P, Zeng H, Poh CF, Ng S, et al. Simple device for the direct visualization of oral-cavity tissue fluorescence. J Biomed Opt. 2006; 11:024006. [PubMed: 16674196]
7. Roblyer D, Kurachi C, Stepanek V, Williams MD, El-Naggar AK, Lee JJ, et al. Objective detection and delineation of oral neoplasia using autofluorescence imaging. Cancer Prev Res. 2009; 2:423–431.
8. Poh CF, MacAulay CE, Laronde DM, Williams PM, Zhang L, Rosin MP. Squamous cell carcinoma and precursor lesions: diagnosis and screening in a technical era. Periodontology 2000. 2011; 57:73–88. [PubMed: 21781180]
9. Poh CF, Zhang L, Anderson DW, Durham JS, Williams PM, Priddy RW, et al. Fluorescence visualization detection of field alterations in tumor margins of oral cancer patients. Clin Cancer Res. 2006; 12:6716–6722. [PubMed: 17121891]
10. Poh CF, MacAulay CE, Zhang L, Rosin MP. Tracing the “at-risk” oral mucosa field with autofluorescence: Steps toward clinical impact. Cancer Prev Res. 2009; 2:401–404.

11. Thomas GT, Lewis MP, Speight PM. Matrix metalloproteinases and oral cancer. Oral Oncol. 1999; 35:227–233. [PubMed: 10621841]
12. Müller MG, Valdez TA, Georgakoudi I, Backman V, Fuentes C, Kabani S, et al. Spectroscopic detection and evaluation of morphologic and biochemical changes in early human oral carcinoma. Cancer. 2003; 97:1681–1692. [PubMed: 12655525]
13. Pavlova I, Williams M, El-Naggar A, Richards-Kortum R, Gillenwater A. Understanding the biological basis of autofluorescence imaging for oral cancer detection: High-resolution fluorescence microscopy in viable tissue. Clin Cancer Res. 2008; 14:2396–2404. [PubMed: 18413830]
14. Pavlova I, Weber CR, Schwarz RA, Williams M, El-Naggar A, Gillenwater A, et al. Monte Carlo model to describe depth selective fluorescence spectra of epithelial tissue: Applications to diagnosis of oral precancer. J Biomed Opt. 2008; 13:064012. [PubMed: 19123659]
15. Scheer M, Neugebauer J, Derman A, Fuss J, Drebber U, Zoeller JE. Autofluorescence imaging of potentially malignant mucosa lesions. Oral Surg Oral Med Oral Path Oral Radiol Endodontol. 2011; 111:568–577.
16. Awan KH, Morgan PR, Warnakulasuriya S. Evaluation of an autofluorescence based imaging system (VELscope™) in the detection of oral potentially malignant disorders and benign keratoses. Oral Oncol. 2011; 47:274–277. [PubMed: 21396880]
17. Maitland KC, Gillenwater AM, Williams MD, El-Naggar AK, Descour MR, Richards-Kortum RR. *In vivo* imaging of oral neoplasia using a miniaturized fiber optic confocal reflectance microscope. Oral Oncol. 2008; 44:1059–1066. [PubMed: 18396445]
18. Haxel BR, Goetz M, Kiesslich R, Gosepath J. Confocal endomicroscopy: A novel application for imaging of oral and oropharyngeal mucosa in human. Eur Arch Otorhinolaryngol. 2010; 267:443–448. [PubMed: 19590883]
19. Muldoon TJ, Roblyer D, Williams MD, Stepanek VMT, Richards-Kortum R, Gillenwater AM. Noninvasive imaging of oral neoplasia with a high-resolution fiber-optic microendoscope. Head Neck. 2011; 34:305–312. [PubMed: 21413101]
20. Roblyer D, Richards-Kortum R, Sokolov K, El-Naggar AK, Williams MD, Kurachi C, et al. Multispectral optical imaging device for *in vivo* detection of oral neoplasia. J Biomed Opt. 2008; 13:024019. [PubMed: 18465982]
21. Pierce MC, Yu D, Richards-Kortum R. High-resolution fiber-optic microendoscopy for *in situ* cellular imaging. J Vis Exp. 2011; 47 http://www.jove.com/index/Details.stp?ID=2306.
22. Wainwright M. Acridine – a neglected antibacterial chromophore. J Antimicrobial Chemotherapy. 2001; 47:1–13.
23. Polglase AL, McLaren WJ, Skinner SA, Kiesslich R, Neurath MF, Delaney PM. A fluorescence confocal endomicroscope for *in vivo* microscopy of the upper- and lower-GI tract. GastrointestEndosc. 2005; 62:686–695.
24. Janssen PA, Selwood BL, Dobson SR, Peacock D, Thiessen PN. To dye or not to dye: A randomized, clinical trial of a triple dye / alcohol regime versus dry cord care. Pediatrics. 2003; 111:15–20. [PubMed: 12509548]
25. Barnes, L.; Eveson, JW.; Reichart, P.; Sidransky, D., editors. Pathology and genetics of head and neck tumors. Lyon: IARC Press; 2005. World Health Organization Classification of tumours.
26. Thomson PJ, Hamadah O, Goodson ML, Cragg N, Booth C. Predicting recurrence after oral precancer treatment: Use of cell cycle analysis. Br J Oral Maxillo Surg. 2008; 46:370–375.
27. Torres-Rendon A, Roy S, Craig GT, Speight PM. Expression of Mcm2, geminin and Ki67 in normal oral mucosa, oralepithelial dysplasias and their corresponding squamous-cellcarcinomas. Br J Cancer. 2009; 100:1128–1134. [PubMed: 19293805]
28. Montebugnoli L, Badiali G, Marchetti C. Prognostic value of Ki67 from clinically and histologically ‘normal’ distant mucosa in patients surgically treated for oral squamous cell carcinoma: a prospective study. Int J Oral MaxilloSurg. 2009; 38:1165–1172.
29. De Oliveira LR, Ribeiro-Silva A, Zucoloto S. Prognostic impact of p53 and p63 immunoexpression in oral squamous cell carcinoma. J Oral Path Med. 2007; 36:191–197. [PubMed: 17391296]

30. Lo Muzio L, Campisi G, Farina A, Rubini C, Pastore L, Giannone N, et al. Effect of p63 expression on survival in oral squamous cell carcinoma. Cancer Investigation. 2007; 25:464–469. [PubMed: 17882659]

31. Saintigny P, El-Naggar AK, Papadimitrakopoulou V, Ren H, Fan Y-H, Feng L, et al. ΔNp63 overexpression, alone and in combination with other biomarkers, predicts the development of oral cancer in patients with leukoplakia. Clin Cancer Res. 2009; 15:6284–6291. [PubMed: 19773378]

32. Moergel M, Abt E, Stockinger M, Kunkel M. Overexpression of p63 is associated with radiation resistance and prognosis in oral squamous cell carcinoma. Oral Oncol. 2010; 46:667–671. [PubMed: 20656547]

33. Ladstein RG, Bachmann IM, Straume O, Akslen LA. Ki-67 expression is superior to mitotic count and novel proliferation markers PHH3, MCM4 and mitosin as a prognostic factor in thick cutaneous melanoma. BMC Cancer. 2010; 10:140. [PubMed: 20398247]

34. Uedo N, Iishi H, Tatsuta M, Yamada T, Ogiyama H, Imanaka, et al. A novel videoendoscopy system by using autofluorescence and reflectance imaging for diagnosis of esophagogastric cancers. GastrointestEndosc. 2005; 62:521–528.

35. Bradley G, Odell EW, Raphael S, Ho J, Le HW, Benchimol S, et al. Abnormal DNA content in oral epithelial dysplasia is associated with increased risk of progression to carcinoma. Br J Cancer. 2010; 103:1432–1442. [PubMed: 20859287]

36. Guillaud M, Zhang L, Poh C, Rosin MP, MacAulay C. Potential use of quantitative tissue phenotype to predict malignant risk for oral premalignant lesions. Cancer Res. 2008; 68:3099–3107. [PubMed: 18451134]

37. Rosin MP, Cheng X, Poh C, Lam WL, Huang Y, Lovas J, et al. Use of allelic loss to predict malignant risk for low-grade oral epithelial dysplasia. Clin Cancer Res. 2000; 6:357–362. [PubMed: 10690511]

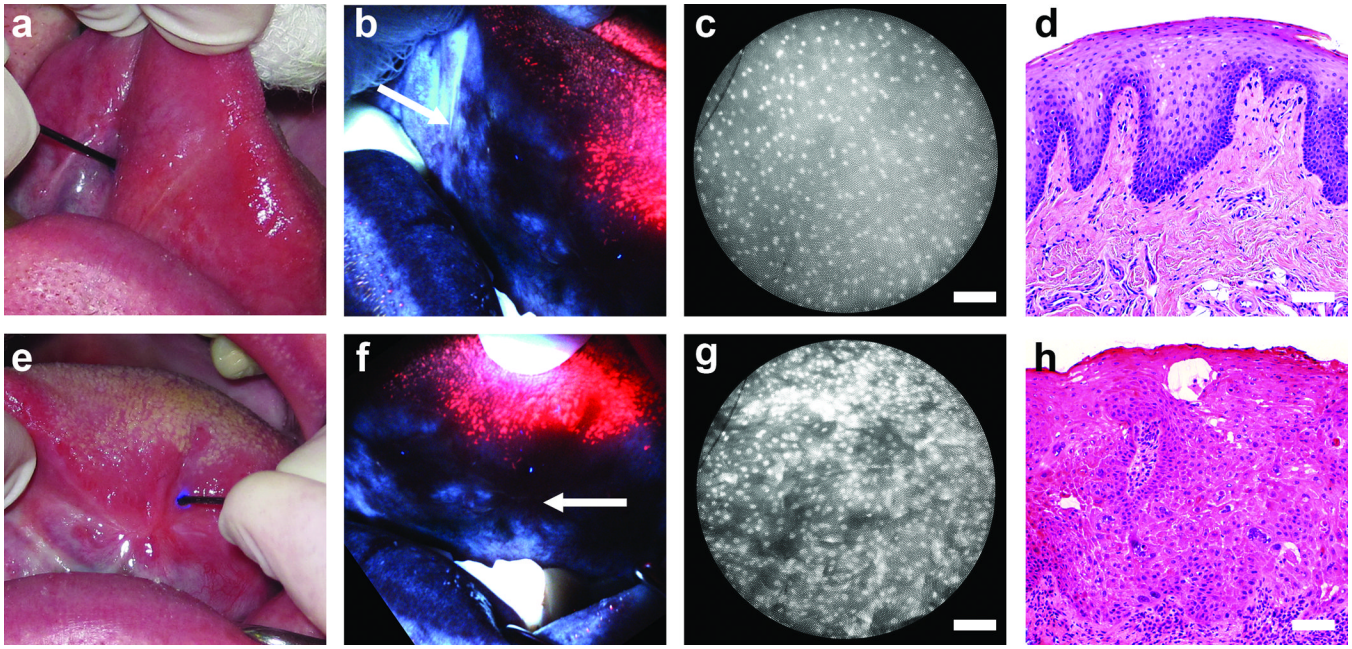

Figure 1.
Multi-modal optical imaging in the oral cavity. (a-d) A normal site on the anterior tongue. (e-h) A site diagnosed with severe dysplasia on the left mid tongue in the same patient. (a,e) White light examination, (b,f) autofluorescence imaging, (c,g) high-resolution microendoscopy, and (d,h) histopathology sections. In (e), scar tissue is apparent, with the smaller lesion alongside. In (b) and (f), arrows indicate the location of the microendoscope probe, as seen in (a) and (e). Scale bars represent 100 μm.

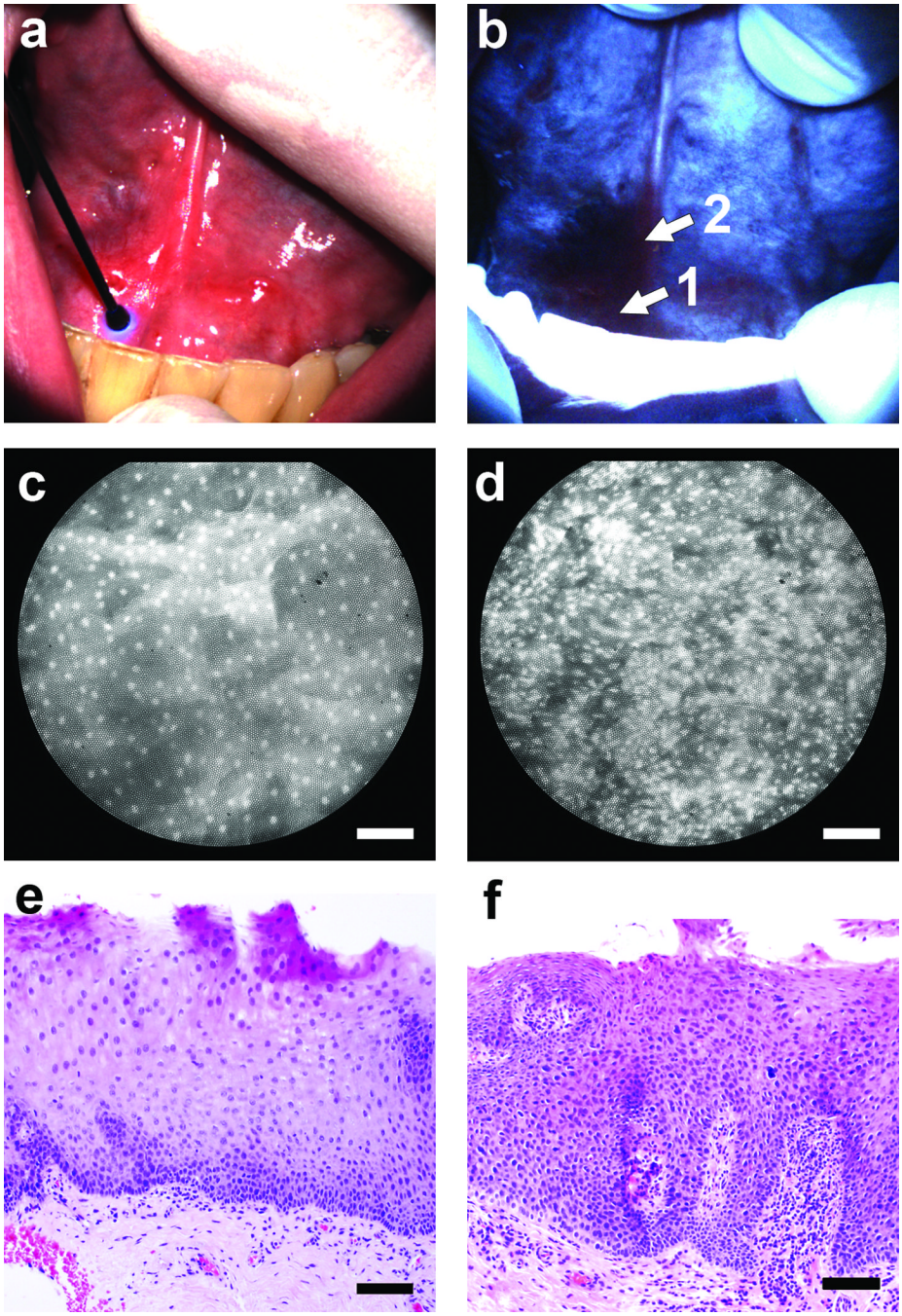

Figure 2.
Multi-modal optical imaging at the floor-of-mouth. (a) The entire area appeared normal on clinical examination. (b) Autofluorescence imaging revealed a region with distinct loss of fluorescence intensity at the patient's right side. (c,d) High-resolution microendoscope images with the probe placed at sites "1" and "2" in panel (b), respectively. (e,f) Histopathology sections from sites "1" and "2" in panel (b). Scale bars represent 100 μm.

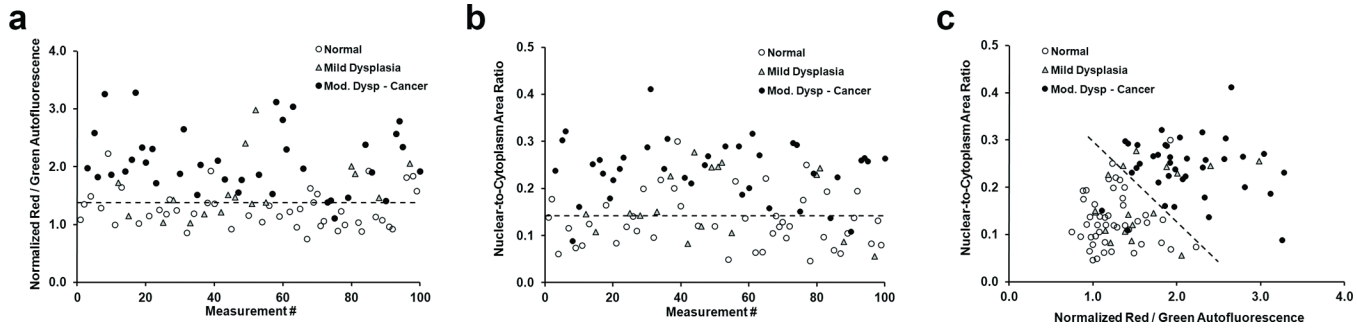

Figure 3.

Quantification of AFI and HRME images. Symbols represent the diagnosis for each site according to pathology. (a) Normalized ratio of red-to-green autofluorescence intensity at each of the 100 sites measured in the study. (b) Nuclear-to-cytoplasm area ratio for the same 100 sites shown in (a). (c) Classification of measurement sites using both wide-field autofluorescence and high-resolution morphology. Dashed lines represent linear threshold values to discriminate between normal sites, and those with mild / moderate / severe dysplasia or cancer.

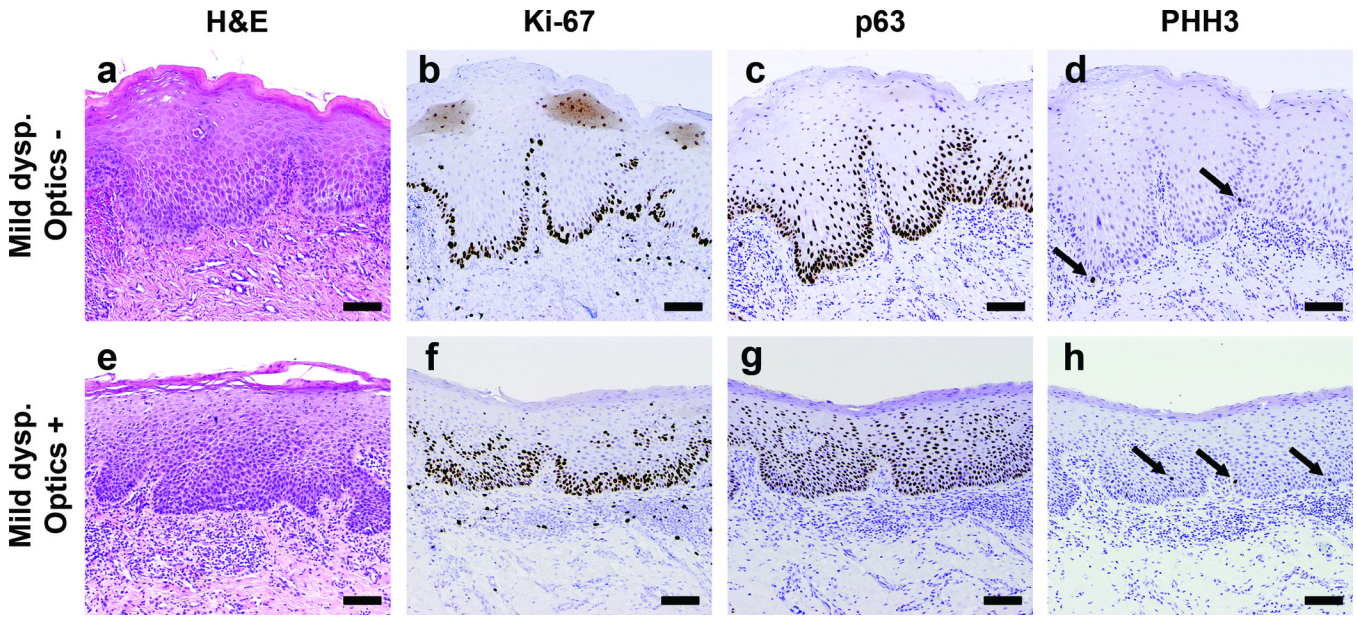

Figure 4.

Histopathology sections of tissue from two sites with a diagnosis of mild dysplasia. (a-d) Sections from a site which was classified as “normal” by optical measurement. (e-h) Sections from a site classified as “abnormal” by optical measurement. (a,e) H&E stained sections used by the study pathologist to classify each site as mild dysplasia. Immunostained sections from the same sites with (b) Ki-67, graded low, (c) p63, low (d) PHH3, low, (f) Ki-67, moderate, (g) p63, high, (h) PHH3, high. Scale bars represent 100 μm.

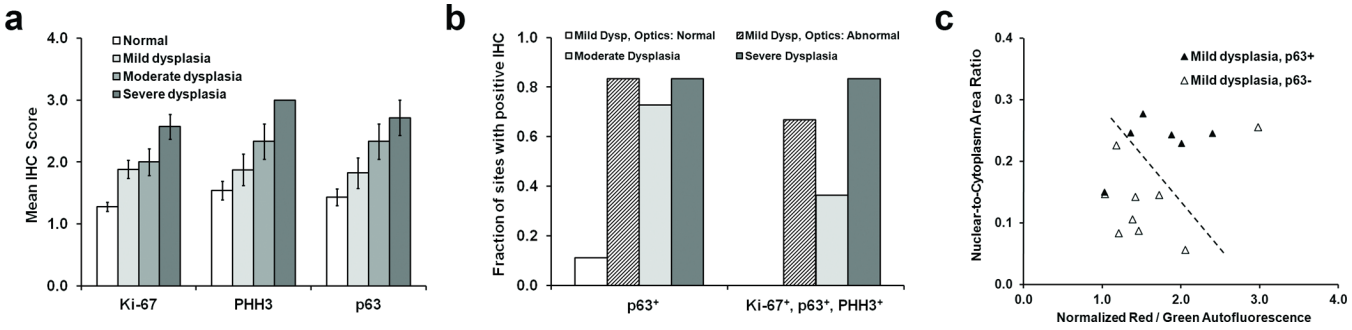

Figure 5.

Analysis of IHC staining of sections from tissue sites with a pathology diagnosis of normal or dysplasia. (a) Mean IHC score (see main text for details) versus pathology grade established by H&E staining, for each of the markers Ki-67, PHH3, and p63. Error bars represent standard errors. (b) The fraction of tissue sites with a positive IHC score for either p63 alone, or for the complete panel of markers tested (see text for definition). Data are shown separated by the pathology grade established by H&E staining. (c) Plot of wide-field autofluorescence and high-resolution N/C ratio values for sites with a pathology diagnosis of mild dysplasia, stratified by p63 status. Note that 15 out of the original 17 measurement sites are displayed due to IHC processing artifacts in 2 cases. The dashed line represents the linear threshold shown in Fig. 5 to discriminate between normal sites, and those with mild / moderate / severe dysplasia or cancer.

Table 1

Percentage of sites accurately classified by optical imaging for each pathologic grade. Data are presented for all sites with mild dysplasia by standard histopathology considered “abnormal”, and also following stratification of those mild dysplasia sites by biomarker status (p63- considered “normal”, p63+ considered abnormal).

	Pathology grade			
	Normal	Mild dysplasia		Mod. Dysplasia - Cancer
		Histopathology	IHC stratified	
AFI alone	76%	65%	67%	97%
HRME alone	71%	65%	73%	92%
AFI + HRME (MMIS)	98%	35%	87%	95%

AFI: Autofluorescence imaging, HRME: High-resolution microendoscopy, MMIS: Multi-modal imaging system (AFI combined with HRME).